Phase-Separation Process in a Poly(methyl methacrylate)-Modified Epoxy System: A Novel Approach to Understanding the Effect of the Curing Temperature on the Final Morphology

D. Olmos, A. Loayza, J. González-Benito

Departamento de Ciencia e Ingeniería de Materiales e Ingeniería Química, Universidad Carlos III de Madrid, Avenida Universidad 30, 28911, Leganés, Madrid, Spain

Received 14 April 2009; accepted 4 July 2009
DOI 10.1002/app.31060
Published online 27 April 2010 in Wiley InterScience (www.interscience.wiley.com).

ABSTRACT: In this study, the physical and chemical changes of a poly(methyl methacrylate) (PMMA)-modified epoxy system were examined to understand the effect of the curing conditions on its final morphology. The curing process of the PMMA–epoxy reactive system was complementarily analyzed by Fourier transform infrared spectroscopy in the near range (FT-NIR) and fluorescence spectroscopy. The relationships among (1) the chemical conversion of the curing reaction, (2) the first moment of the fluorescence emission band ($\langle\nu\rangle$) arising from a chromophore chemically bonded to the epoxy reactive system, (3) the phase-separation process, and (4) the dynamics of the epoxy thermoset during its curing process are discussed. From a chemical point of view, FT-NIR did not reveal any significant change in the curing reaction with the presence of 2 wt % PMMA. However, in terms of physical changes, the analysis of the fluorescence response clearly showed variations in the curing reaction due to the presence of the thermoplastic polymer. Also, fluorescence allowed the estimation of the glass-transition temperature of the system with curing when the reaction was diffusion-controlled, whereas Fourier transform infrared spectroscopy was not sensible enough. In the second part of this study, scanning electron microscopy images of the PMMA-modified epoxy system were analyzed to understand the effect of the temperature on the final morphology when the amount of thermoplastic was below the critical volume fraction. A linear dependence between the inverse of the mean area of the thermoplastic-rich domains and the inverse of the absolute temperature was obtained. J Appl Polym Sci 117: 2695–2706, 2010

Key words: blends; curing of polymers; fluorescence; FT-IR

INTRODUCTION

The importance of polymer blends is associated with the variety of properties that can be achieved with them. In particular, modified epoxy thermosets have been the main topic of many studies in the last 3 decades.[1] In general, the addition of high or relatively high-glass-transition-temperature (T_g) thermoplastics to epoxy systems has been considered to increase their toughness, improve their poor resistance to crack propagation, retain a high T_g, and reduce thermal stresses.[1–4] In these modified epoxy thermosets, the morphology is a significant factor influencing their properties.[1,5–9] However, a general method for preparing material with a particular composition of modifier to obtain a certain morphology that leads to maximum property enhancement required for a specific application are not known yet. Because of this, the understanding and even control of the necessary conditions to obtain those specific morphologies is greatly needed.

During the curing reaction of a thermoplastic-modified epoxy resin, the oligomeric species might be more compatible with the modifier than with the reactive monomers.[10–12] However, in many cases, phase separation occurs after a certain reaction time. This reaction-induced phase separation depends on the nature of the reactive components and the thermoplastic modifier. Therefore, the curing conditions and the initial composition of the blend[1,5] should be the main aspects to take into account when one designs this sort of material with a particular morphology.

It is well known that a transition of several morphologies is expected and depends on several factors: (1) a thermoset-rich continuous phase structure when the thermoplastic concentration is lower than

Correspondence to: J. González-Benito (javid@ing.uc3m.es).

Contract grant sponsor: Ministerio de Ciencia e Innovación of Spain and the Comunidad de Madrid; contract grant numbers: MAT2007-61607, HH2006-0007, UC3M-TM-05-053, MAT2004-20893-E, S-0505/MAT/0227.

the critical volume fraction ($\Phi_{TP,crit}$) and/or when the phase-separation rate is much faster than the curing reaction rate, (2) a bicontinuous structure near $\Phi_{TP,crit}$ when the phase-separation rate is similar to the curing reaction rate, and (3) a thermoplastic-rich continuous phase mainly when the thermoplastic concentration is higher than $\Phi_{TP,crit}$. Previous studies[13] have shown that $\Phi_{TP,crit}$, does not vary significantly with conversion. Therefore, to obtain a morphology in which the maximum amount of thermoplastic forms a solution with a thermoset, the composition of the blend should be, at least, lower than $\Phi_{TP,crit}$. Once the composition is fixed, apart from the nature of the reactive components, the curing conditions should be the only factor responsible for a particular morphology.

In this study, poly(methyl methacrylate) (PMMA) was chosen as a model thermoplastic modifier because of its initial homogeneous dissolution with diglycidyl ether of bisphenol A (DGEBA) over the entire composition range.[14,15] Also, much information can be easily compiled because PMMA has been widely studied by several authors under different conditions. For instance, several studies[14,16,17] have shown that the final morphologies and properties of epoxy–PMMA cured blends depend on the curing agent used. In this context, Remiro et al.[17] studied the transparency of PMMA-modified epoxy (DGEBA) using 4,4′-methylene dianiline as a hardener. They noticed that the phase-separation process and, consequently, the size of the dispersed domains depended on the curing conditions.

On the other hand, in other systems, several authors have analyzed the influence of the curing conditions on the resulting morphologies. In most rubber-modified epoxy systems, the analysis of the experimental results showed different tendencies in the mean diameter ($\langle D \rangle$) of the dispersed-phase particles as a function of temperature.[18] For example, it has been reported that the mean particle size of the dispersed domains can be linearly correlated with the viscosity of the system at the cloud point, which shows a negative slope. As the viscosity decreases when the temperature increases, this correlation reflects the observed increase of $\langle D \rangle$ of the dispersed-phase particles with the precuring temperature.[19]

However, despite the existence of a vast amount of literature related to those aspects, the mechanism by which a particular morphology is obtained is not yet completely understood. Therefore, if a theoretical model or at least semiempirical equations were proposed, tailored morphologies for this kind of system could be obtained. To do this, information about the physicochemical changes appearing throughout the curing process should be obtained. However, to obtain this information experimentally, *in situ*, and nondestructively is very difficult. The use of fluorescence might be the answer.

In the curing of diepoxy–diamine systems, the relation between T_g and the conversion of the epoxy monomer (α) is critical to the deep understanding of the physicochemical processes occurring within the reactive mixture. Furthermore, to optimize the conditions of curing for thermosetting materials, to monitor simultaneously, nondestructively, and *in situ*, both the chemical conversion and changes in T_g or any other parameter directly related to it would be very helpful. Although several techniques have been used to monitor the curing process in epoxy-based materials, Fourier transform infrared (FTIR) spectroscopy[20–25] and differential scanning calorimetry (DSC)[26–30] have probably been the most widely used. However, none of these studies have achieved the objective of nondestructively monitoring the curing process and determining in every moment either the value of the T_g of the system or any parameter directly related to it. The use of fluorescence might be a possibility.

The fluorescence emission from many molecules or groups (fluorophores) is so sensitive to changes in their immediate surroundings that very small amounts of them are enough to obtain much information. In general, the fluorescence emission changes when polarity and/or rigidity variations occur in the system where the fluorophore is immersed.[31–40] For example, there has been an important amount of work done with fluorescence to follow polymerization processes.[24,25,36,41–52] In some studies, it has been proposed that during the polymerization, an enhancement in the microviscosity of the medium exists, which leads to a decrease in nonradiative decay rate and, consequently, an increase in the fluorescence quantum yield.[36] Other researchers have used the increase in the fluorescence intensity that comes from the chemical changes of an intrinsic fluorophore.[41,42] However, these methods have as a main limitation the fact that they do not eliminate the effect of intensity variations that arise from external factors. Because of this fact, new methods for fluorescence analysis have been used to monitor polymerization processes. Neckers and coworkers[43,44] reported the use of fluorescence probes for monitoring the curing process of polyacrylate monomers with an intensity ratio method, whereas Lemmetyinen and coworkers[45,46,53] developed an intensity ratio method where ratios of the low- to high-intensity changes in the emission bands were used to determine the degree of curing. Rigail-Cedeño and Sung[54] correlated the intrinsic fluorescence intensity changes due to quenching by aliphatic amines to the extent of the epoxy reaction, or the epoxy conversion, obtained by IR spectroscopy (α_{IR}). However, although this method seems to

be very promising, mainly for monitoring the curing process at long times or postcuring processes, quantitative analysis of the curing characterization based on this method does not seem to be possible. González-Benito and coworkers[24,25,37,47,53,55] reported a new method for accurately monitoring polymerizations. This method is based on the use of $\langle\nu\rangle$ [$\langle\nu\rangle = \Sigma I_F(\nu_F)\nu_F/\Sigma I_F(\nu_F)$, where $I_F(\nu_F)$ is the fluorescence intensity at a specific wave number ν_F].[47] This photophysical parameter has been used recently, even to carry out kinetic studies of curing processes, for instance, in the case of polyurethanes[53] and epoxy systems.[25] Taking into account that any fluorophore has more or less stabilization of its excited estate when any change (rigidity, polarity, etc.) happens in its immediate surroundings, a shift of the fluorescence emission is always expected.

Pascault and Williams[56] analyzed different equations that were proposed to fit T_g experimental data versus conversion. However, it would be interesting to find new parameters also related to the T_g of the system and that could be measured easily *in situ,* nondestructively, and in real time during the curing process. Here, we propose $\langle\nu\rangle$ of a fluorophore chemically bonded to the reactive system.

The aim of this study was to understand the conditions required to obtain specific morphologies in thermoplastic-modified epoxy thermosets. To carry this out (1) nondestructively and *in situ,* monitorization of the physical and chemical changes of a PMMA-modified epoxy system was performed, and (2) the morphologies of the blends under different curing conditions were analyzed. The curing process of the PMMA–epoxy reactive system was complementarily analyzed by Fourier transform infrared spectroscopy in the near range (FT-NIR) and fluorescence spectroscopy, whereas the morphologies were studied from image analysis of obtained scanning electron microscopy (SEM) micrographs.

EXPERIMENTAL

Materials and sample preparation

Poly(bisphenol A-*co*-epichlorohydrin) glycidyl endcapped [**I;** DGEBA, Aldrich Co. (Milwaukee, WI; St. Fallavier, France); number-average molecular weight = 348 g/mol (n = 0.03)] was labeled with a dansyl fluorophore with 5-dimethylaminonaphthalene-1-(2-aminopenthyl) sulfonamide (**II;** Aldrich; Allentown, PA; St. Fallavier, France); we followed a previously described procedure,[47] for which a naphthalene sulfonamide/epoxy ratio lower than 10^{-5} mol/kg was achieved.

A model thermoplastic-modified epoxy system, epoxy–PMMA, was prepared by the blending of PMMA (**III;** Polysciences, Inc., Warrington, PA), with a number-average molecular weight of 75,000 and a polydispersity of 2.8, with a stoichiometric mixture of dansyl, labeled DGEBA, and 1,5-diamino-2-methylpentane (DAMP; **IV;** Fluka Chemika, Buchs, Switzerland). The composition studied for the modified epoxy system was 2 wt % PMMA. Furthermore, as a control sample, labeled DGEBA–DAMP without PMMA was prepared under the same conditions (neat epoxy system):

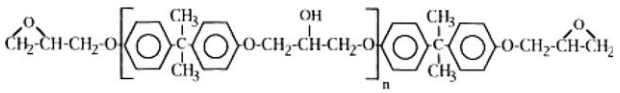

I

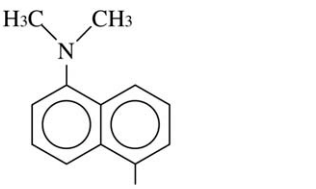

II

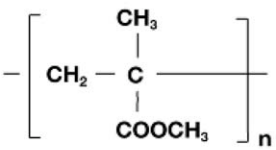

III

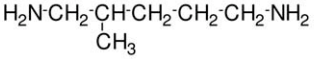

IV

The preparation of the initial reactive mixtures with and without PMMA was already described elsewhere.[55] All of the reactive mixtures were cured at different temperatures (50, 60, 70, and 80°C), and we stopped the reaction when almost a constant value of conversion was reached.

Instrumentation

The curing process was followed by (1) FT-NIR and Fourier transform infrared spectroscopy in the medium range (FT-MIR) and (2) steady-state fluorescence spectroscopy.

The FT-NIR and FT-MIR spectra were recorded with an FTIR Spectrum GX (PerkinElmer, Norwalk, CT) with a homemade program to collect spectra as a function of time. A resolution of 4 cm^{-1} and five scans were used. The curing reaction was monitored at 50, 60, 70, and 80°C in an oven with a temperature controller (±0.5°C; Specac, Cranston, RI; Orpington, Kent, UK).

The fluorescence spectra were recorded in a steady state fluorimeter FS 900 from Edinburgh Instruments (Livingston, UK) with an optical fiber cable for both exciting and collecting the

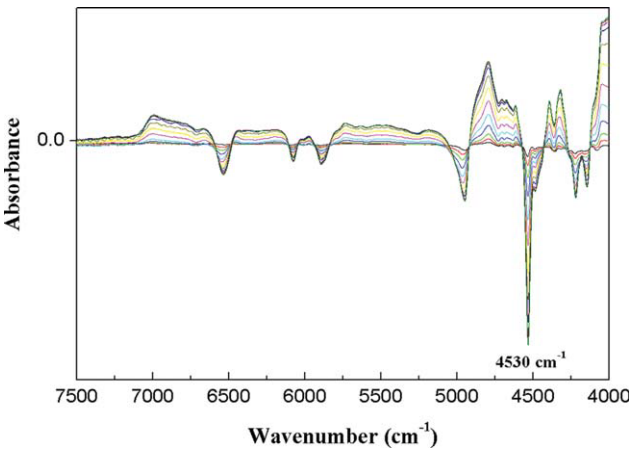

Figure 1 Evolution of the FT-NIR spectra for the DGEBA–DAMP reactive mixture at 50°C in terms of the difference between the spectra at different curing times and the spectrum at the beginning of the curing process. [Color figure can be viewed in the online issue, which is available at www.interscience.wiley.com.]

fluorescence. As in the FT-NIR experiment, between two microscope-glass plates, the fluorescent sample was located inside the oven. The excitation and emission slits were set at 2 and 5 mm, respectively, which corresponded to band passes of 1.8 and 4.5 nm, respectively. All the spectra were recorded with only one scan between 360 and 650 nm, with the excitation wavelength set at 340 nm and a dwell time of 0.1 s selected. As in the case of FT-NIR, the curing reaction was monitored at 50, 60, 70, and 80°C.

Finally, to visualize the effect of the precuring temperature on the final morphology, a Philips XL30 (FEI, Hillsboro, OR) scanning electron microscope was used. Before the SEM examination, the fully cured samples were freeze-fractured, immersed in chloroform for 24 h to selectively dissolve the PMMA-rich phase domains, dried overnight *in vacuo* to eliminate any trace of solvent that could remain in the sample, and finally, gold-coated to make the samples conductive and to prevent charge accumulation over the surface during SEM observation. The images analysis was performed with the program IMAGE-PRO PLUS, version 5.0 (Media Cybernetics, Inc., Bethesda, MD).

RESULTS AND DISCUSSION

As an example, in Figure 1 the results of the differences between the spectra of the DGEBA–DAMP reactive mixture at different curing times and the spectrum at a curing time of $t = 0$ are presented. In particular, the evolution of the FT-NIR spectra for curing at 50°C is shown (Fig. 1). For the PMMA-modified sample and the rest of temperatures considered, similar results were obtained. The negative peaks in Figure 1 indicate the bands that disappeared, whereas the positive peaks show the bands that appeared during the curing process.

The disappearance of the band at 4530 cm^{-1}, which is usually assigned to the overtone of oxirane ring stretching,[21] was clearly shown. Although other negative peaks related to the consumption of epoxy groups are also shown in Figure 1, as that at 6065 cm^{-1}, in this study, the peak used to monitor the epoxy group's evolution was the one centered at 4530 cm^{-1} because it did not overlap with other peaks and thus provided a direct means of monitoring the epoxy concentration.

The extent of the reaction at any time t obtained from the FT-NIR spectra (α_{IR}) was calculated in terms of the epoxy group absorption according to the following equation:

$$\alpha_{IR} = 1 - \frac{(A_{E,t}A_{R,0})}{(A_{E,0}A_{R,t})} \quad (1)$$

where $A_{E,0}$ and $A_{R,0}$ are the initial areas of the epoxy and reference bands, respectively, and $A_{E,t}$ and $A_{R,t}$

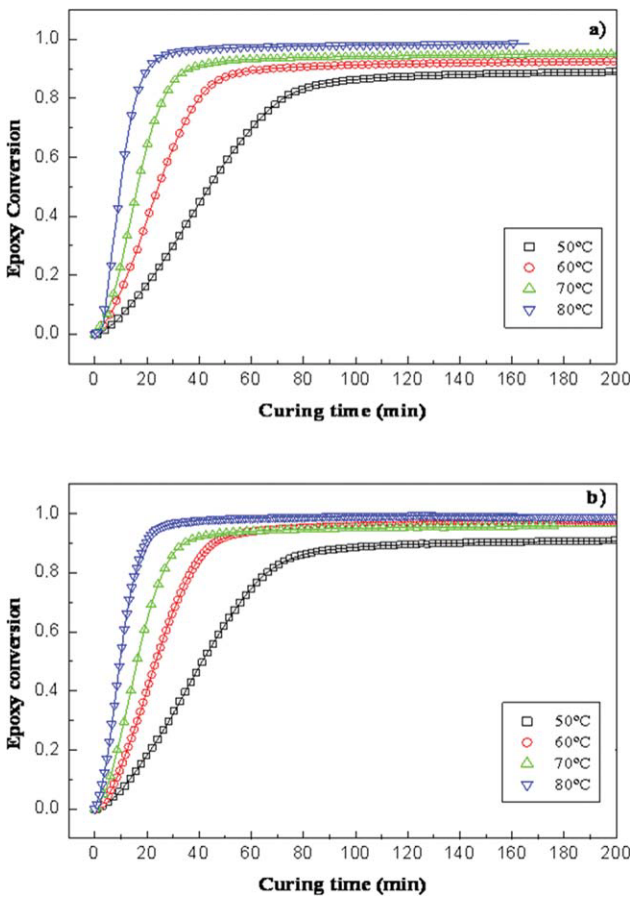

Figure 2 Epoxy group conversion versus the curing time obtained from FT-NIR data analysis at different temperatures: (a) DGEBA–DAMP and (b) DGEBA–PMMA. [Color figure can be viewed in the online issue, which is available at www.interscience.wiley.com.]

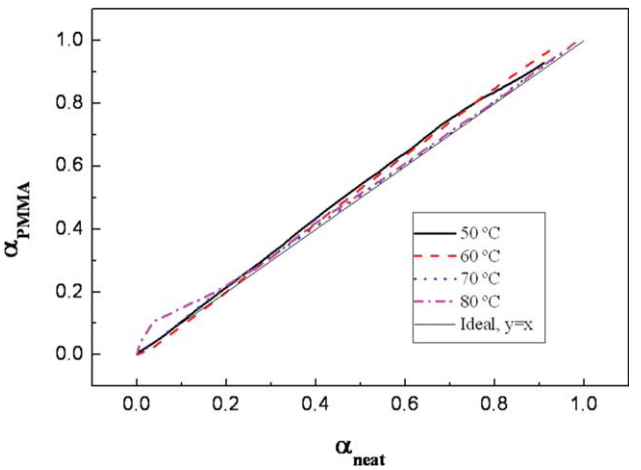

Figure 3 Comparison at specific curing times between α_{neat} and α_{PMMA}. [Color figure can be viewed in the online issue, which is available at www.interscience.wiley.com.]

are to the areas of the same bands at a certain time t. The area of the band at 4530 cm^{-1} was used to monitor the disappearance of the epoxy group, and the area of the band at 4623 cm^{-1}, due to a combination of C—H stretching vibrations of the benzene ring, was used as the reference.[21]

For the neat and PMMA-modified epoxy systems, α_{IR} as a function of curing time at different temperatures is represented in Figure 2. In both cases, typical sigmoidal plots usually obtained for this kind of systems[20,21] were observed; this suggested a sequence of three steps during the curing reaction: (1) the beginning of the reaction with a moderate reaction rate, (2) an autoacceleration step due to an increase of local concentration of the reactive groups and autocatalysis with a fast or relatively fast reaction rate, and (3) a region in which the mobility of the reactive groups was so restricted that the reaction was almost stopped and the reaction rate trended toward zero. Also as expected, in Figure 2, it is shown that the reaction rate increased with temperature.

On the other hand, when we compared the results from the neat epoxy system with those of the modified one (Fig. 3), it was possible to observe that independently of the temperature, the reaction seemed to go slightly faster when PMMA was present in the system, at least with the concentration used in this study and for conversions lower than 0.8. Figure 3 represents, at specific curing times, the values of epoxy conversion for the neat epoxy system (α_{neat}) versus the values of epoxy conversion for the PMMA-modified epoxy system (α_{PMMA}). These plots could be fitted to straight lines with slopes almost equal to 1. Therefore, at least from a chemical point of view, the presence of the PMMA in such a low concentration did not modify the epoxy–amine reaction rate. It is important to highlight that the data represented in Figure 3 came from the best fits of the curves (solid lines) represented in Figure 2. Those fits were performed by a nonlinear curve fitting with the function given by the following equation:

$$\alpha_{IR} = \sum_{i=1}^{i=\infty} a_i \frac{t^{n_i}}{b_i^{n_i} + t^{n_i}} \quad (2)$$

where t is the curing time and a_i, b_i, and n_i are fitting parameters. As shown by the solid lines in Figure 2, the fits were really good along the whole curves. In fact, the average deviation from the real data was lower than 0.01%.

On the other hand, the curing process of both systems was also monitored by fluorescence as described elsewhere.[55] The variation of the first moment of the dansyl emission band throughout the curing was found to be clearly dependent on the presence of the PMMA modifier. With a similar data analysis, as in the case of the FTIR results, in Figure 4 the value of the first moment for the neat epoxy system ($\langle\nu\rangle_{neat}$) versus the value of the first moment for the PMMA-modified epoxy system ($\langle\nu\rangle_{PMMA}$) at specific curing times are represented. From these results (Fig. 4), the effect of PMMA on the curing process was clearly observed. This result, therefore, suggests that fluorescence provided more information than a simple chemical evolution of the system under study.

Except for the curing at 80°C, $\langle\nu\rangle$ for the neat epoxy system changed faster with curing when the conversion was lower than 0.5 than for the PMMA-modified system. Also, this effect was more pronounced at higher temperatures. When one considers that in the case of epoxy conversion, practically no differences were observed; only differences in the physical properties of the systems could have been responsible for the curve profiles observed in Figure 4. This result seemed to confirm that

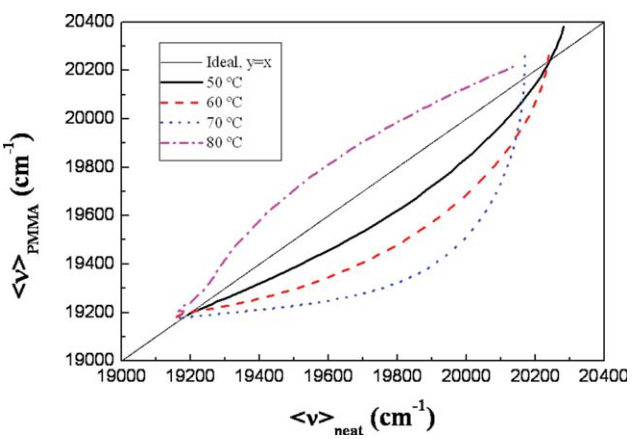

Figure 4 $\langle\nu\rangle_{neat}$ versus $\langle\nu\rangle_{PMMA}$ at different temperatures. [Color figure can be viewed in the online issue, which is available at www.interscience.wiley.com.]

fluorescence gave, in this kind of systems, important information that could not be found with other techniques of analysis (e.g., FTIR, DSC), and that might be crucial to the proper control of the processing during online manufacturing.

It is important to understand which are the real physicochemical changes being monitored when the first moment of the dansyl emission band is used. For instance, if there were a simple relation between the fluorescence response of the dansyl label and the dynamic of the system for a particular curing time or conversion, with a relatively simple fluorescence device, it would be possible to control the online process for manufacturing these epoxy-based materials. Other scientists have considered the same objectives with data obtained from other techniques, such as FTIR and DSC. Pascault and Williams[56] analyzed different equations that were proposed to fit the experimental data of T_g versus chemical α. They found one equation that allowed satisfactory fitting of the results:

$$\frac{(T_g - T_{g0})}{(T_{g\infty} - T_{g0})} = \frac{\lambda\alpha_{IR}}{1-(1-\lambda)\alpha_{IR}} \quad (3)$$

where λ is a fitting parameter and $(T_g - T_{g0})/(T_{g\infty} - T_{g0})$ is the normalized glass-transition temperature variation for a particular epoxy conversion, where T_g, T_{g0}, and $T_{g\infty}$ are the glass-transition temperatures of the system at $\alpha = \alpha$, $\alpha = 0$, and $\alpha = 1$, respectively.

It is well known that the dansyl fluorescence shows an important solvatochromic shift that is highly dependent on the polarity and viscosity of the medium in which it is immersed. Therefore, in reactive systems as the one under consideration, three factors that can affect the emission band shift are expected: (1) the polarity, because of hydroxyl groups formed during the curing process; (2) the rigidity, because there is a viscosity increase due to the curing reaction; and (3) the temperature, because it directly affects the dynamics of the system.

A polarity increase should give a redshift of the emission band, whereas a rigidity increase should give a blueshift.[57] During curing, the results obtained exclusively showed a blueshift, which suggested that the rigidity increase must have been the most important contribution to the values observed for the first moment. Therefore, it was reasonable to consider a direct dependence between the value of the first moment of the emission band and the T_g of the systems because T_g reflects the dynamics of a system and is actually directly related to the rigidity of the system.

The first approach might be to consider a proportional relation between the change in the first moment ($\Delta\langle\nu\rangle$) and the variation of the glass-transition temperature (ΔT_g). This dependence could be described by the following equation:

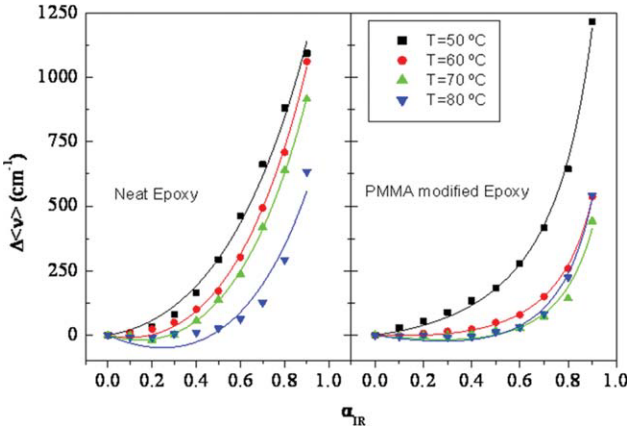

Figure 5 $\Delta\langle\nu\rangle$ as a function of α_{IR}. The solid lines represents the best fits with eq. (4) ($\lambda = 0.5$ for the neat epoxy system and $\lambda = 0.1$ for the PMMA-modified epoxy system). [Color figure can be viewed in the online issue, which is available at www.interscience.wiley.com.]

$$\Delta\langle\nu\rangle = A\frac{(T_g - T_{g0})}{(T_{g\infty} - T_{g0})} \quad (4)$$

where $\Delta\langle\nu\rangle$ is the variation in the first moment at a particular conversion and A is a constant that only depends on the curing temperature.

With the assumption that eq. (4) can describe the curing evolution for this kind of systems like Williams-DiBenedetto [eq. (3)] in terms of chemical conversion, when eq. (3) is substituted into eq. (4), it can be written as

$$\Delta\langle\nu\rangle = A\frac{\lambda\alpha_{IR}}{1-(1-\lambda)\alpha_{IR}} \quad (5)$$

However, for the neat epoxy system, the representation of $\Delta\langle\nu\rangle$ versus α_{IR} cannot be properly fitted with eq. (5). This result suggests that the chemical contribution should be taken into account. If $\Delta\langle\nu\rangle$ due to chemical changes is considered as an additive contribution, the whole $\Delta\langle\nu\rangle$ might be expressed by the following equation:

$$\Delta\langle\nu\rangle = A\frac{\lambda\alpha_{IR}}{1-(1-\lambda)\alpha_{IR}} + B\alpha_{IR} \quad (6)$$

where A and B are constants that account for the weight of each contribution and only depend on the temperature. In this case, relatively good fits were obtained (Fig. 5). In every case, a constant value of 0.5 for λ was used because it was close to those values obtained experimentally for similar systems.[56] In every case, the fitting parameter B was negative as expected because the chemical contribution (polarity

TABLE I
Curing Times and Conversions at Which Phase Separation Took Place for Four Precuring Temperatures

		Techniques and methods		
		Flory–Stockmayer	Average from FT-MIR and fluorescence data[55]	FT-MIR
Epoxy sample		Gel conversion	Curing time (min)	$\langle\alpha_{IR}\rangle$
PMMA-modified	50°C		45	0.6
	60°C	0.58	29	0.6
	70°C		19	0.6
	80°C		12	0.6

α_{IR} is the average infrared conversion in terms of epoxy group conversion.

increase) exerted an opposite effect on the first moment (redshift) with respect to the rigidity increase (blueshift). Now it is necessary to highlight the fact that the data used in Figure 5 were extracted from the curves of $\langle\nu\rangle$ versus curing time and α versus curing time by means of interpolations; therefore, considerable errors, at least when the changes were very fast, as in the case of low conversions at higher temperatures, were expected. This might be the reason why the fit obtained for the experiment at 80°C was not as good as those obtained for the rest of temperatures.

With the assumption, therefore, that eq. (6) describes the fluorescence behavior as a function of conversion, it was now possible to explain the evolution of the A and B parameters with curing temperature. The general tendency observed was that the A/B ratio decreased with temperature (2.21, 1.81, 1.72, and 1.53 for 50, 60, 70, and 80°C, respectively); this suggested that the weight of the chemical contribution increased with curing temperature. This result was reasonable because, for a given conversion, the viscosity reduction due to a high temperature (exponential dependence) may have been enough to balance the viscosity enhancement due to the curing reaction (nonexponential dependence).

For the PMMA-modified epoxy system, similar fits could be done with eq. (6), although in this case, a lower value of λ (0.1) was required to adequately fit the data (Fig. 5). With this system, again the A/B ratio decreased with temperature (19.0, 8.19, 5.55, and 5.51 for 50, 60, 70, and 80°C, respectively) but in a more pronounced way. These results were in accordance with the important effect exerted by PMMA in the dynamics of the epoxy system under study.

With the aforementioned assumptions, from eqs. (3)–(6) one equation can be written that relates $\Delta\langle\nu\rangle$ with ΔT_g:

$$\Delta\langle\nu\rangle = A\Delta T_g + B\frac{\Delta T_g}{\lambda + (1-\lambda)\Delta T_g} \tag{7}$$

The practical implication of this expression might be very important because this new relation between the T_g of the system and $\langle\nu\rangle$ [eq. (7)] would allow estimation of the T_g of the system as a function of curing time when the reaction is diffusion-controlled and FTIR analysis is not sensible enough to the curing changes.

Morphology study

In a previous article,[55] by means of FT-MIR and steady-state fluorescence, the curing times at which phase separation took place were obtained for the four precuring temperatures studied. From the data of epoxy conversion as a function of curing time obtained by FT-NIR, the conversion at which phase separation took place was obtained by interpolation on the curves of Figure 2 (Table I).

In every case, a conversion of 0.6 was obtained, similar to the gel conversion predicted by the Flory–Stockmayer's theory. This near coincidence suggested, therefore, that the very low fraction of PMMA (2% w/w) and its favorable interactions with the epoxy system allowed a large window of miscibility with respect to the epoxy conversion.

Following the scheme to calculate the critical composition described in ref. 58, a value of $\Phi_{TP,crit} = 0.074$ was obtained for the system under study; this was higher than that one used in this study (volume fraction of PMMA $\Phi = 0.018$). Therefore, if one considers that phase separation takes place just in the gel when the viscosity of the system increases to infinity and when the chemical reaction rate starts to level off, a morphology formed by small domains, rich in PMMA, homogeneously distributed in a matrix rich in the epoxy component is expected. The formation of larger domains would require the diffusion of PMMA molecules from longer distances, which would depend on the viscosity of the medium, with the diffusion being more favorable with a lower viscosity.

In Figure 6, the morphologies observed for the PMMA-modified epoxy system at different precuring temperatures used in this study are presented. All of them showed similar morphologies with nearly spherical holes homogeneously distributed on the surface; this reflected the brittle freeze fracture

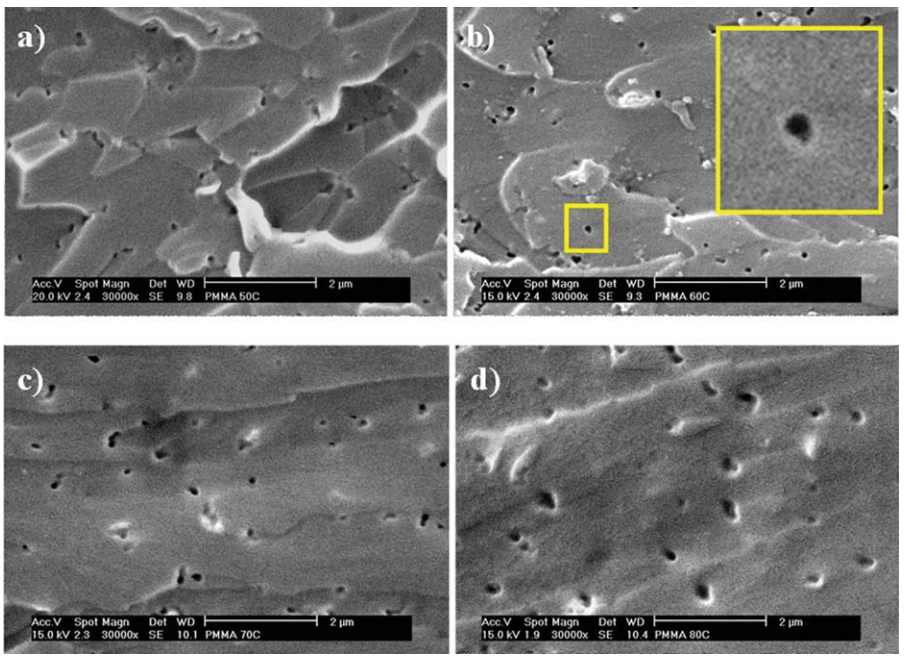

Figure 6 SEM images for freeze-fractured samples of the PMMA-modified epoxy system precured at different temperatures: (a) 50, (b) 60, (c) 70, and (d) 80°C. [Color figure can be viewed in the online issue, which is available at www.interscience.wiley.com.]

of the material. When we took into account that chloroform was used to selectively extract the PMMA, the particular topography observed indicated a morphology formed by nearly spherical PMMA-rich domains homogeneously distributed in an epoxy-rich matrix. It seemed that there existed very small variations in the PMMA domain size and shape as a function of the precuring temperature; however; direct inspection of the images did not seem enough to be completely sure. Because of this fact, analyses of the images were performed.

In the image analysis, two parameters were considered: the domain area, which was the fill area within the borders of the holes left by the extracted PMMA domains [see Fig. 6(b)], and the shape factor (SF), which represented the ratio between the major and the minor axes of the ellipse equivalent for the object under analysis. More than 30 objects were selected from each image to make the statistical analysis.

In Figure 7, as an example, a histogram of bars for the domains size obtained for the sample precured

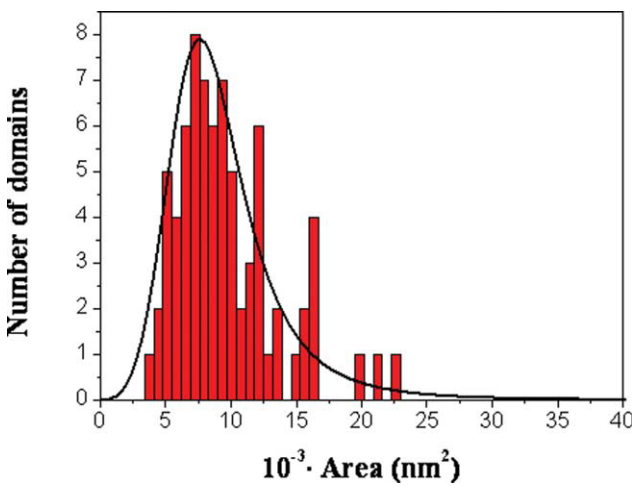

Figure 7 Histogram of the domains size obtained for the sample precured at 60°C. The solid line represents a fit of the domain size distribution. [Color figure can be viewed in the online issue, which is available at www.interscience.wiley.com.]

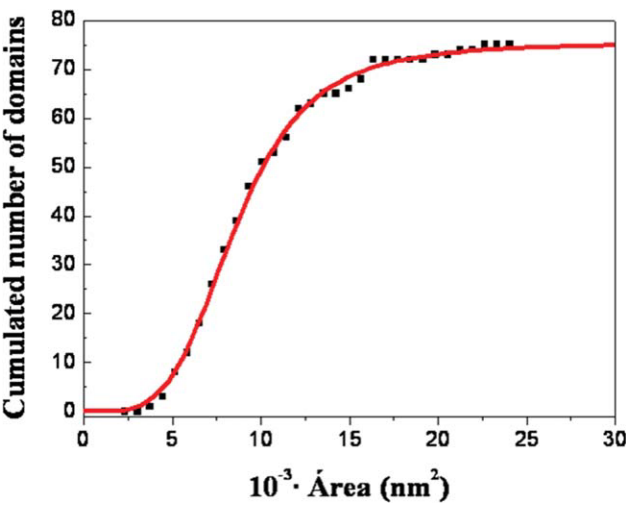

Figure 8 Cumulative curve obtained from the histogram of Figure 7. The solid line represents the best fit with a nonlinear curve fitting with a logistic function. [Color figure can be viewed in the online issue, which is available at www.interscience.wiley.com.]

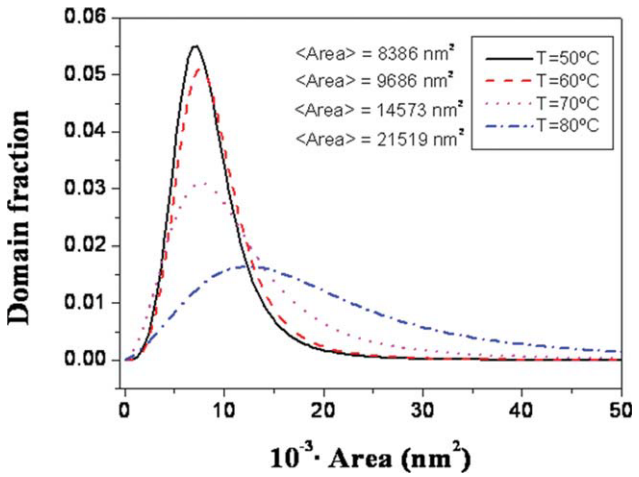

Figure 9 Fitted size distribution curves of the PMMA domains at different temperatures. [Color figure can be viewed in the online issue, which is available at www.interscience.wiley.com.]

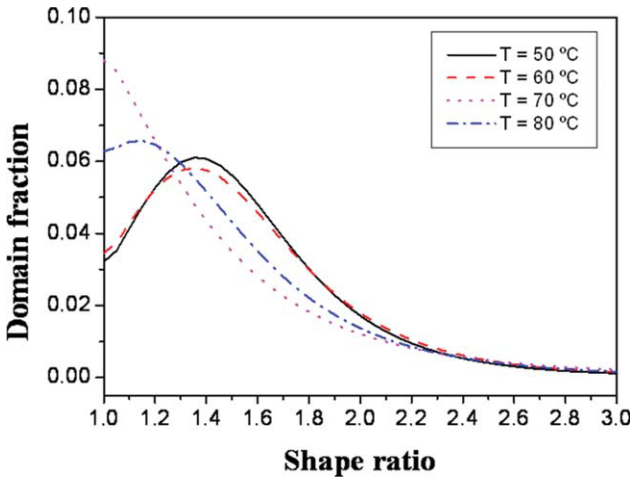

Figure 10 Fitted SF distributions of the PMMA-rich domains at the four precuring temperatures. [Color figure can be viewed in the online issue, which is available at www.interscience.wiley.com.]

at 60°C is shown. Similar results were obtained for the other temperatures. As shown, the distribution obtained was not very smooth; therefore, more objects needed to be analyzed to perform a more accurate analysis. However, we found it possible to indirectly obtain smoother distributions following three steps:

1. First, the convolution of the distribution was obtained; in other words, the cumulative curves for the areas measured were plotted (e.g., Fig. 8).
2. The second step was to fit the cumulative data with a nonlinear method with a logistic function (solid black line in Fig. 8).
3. The last step was to use the fitted cumulative curves to obtain, by deconvolution, curves that fit reasonably well the experimental distributions of the domain sizes obtained (solid line in Fig. 7).

In every case, a coefficient of determination higher than 0.99 was obtained.

For comparison, in Figure 9, the size distribution curves of the PMMA domains at different temperatures are shown. It was observed, as expected from simple inspection of the SEM images (Fig. 6) that on average, the PMMA domain size in the blend increased as the precuring temperature increased. Particularly, a shift of the distribution maximum to larger PMMA-rich domains and a broadening of the distribution when the precuring temperature increased were found. The values of the first moment of the distributions are also included in Figure 9 and show the aforementioned distribution shift with temperature.

Apart from the domain size, another parameter of the morphology that might have affected the final properties of the blends was the SF associated with the PMMA-rich domains. From the analysis of images such as those shown in Figure 6 and with the same method for obtaining the fitted distribution of areas, the distributions of SFs of the PMMA-rich domains were obtained at the four precuring temperatures (Fig. 10). If one considers the position of the distribution maxima, it can be said that on average, from 50 to 70°C, the spherical symmetry of the domains increased, and then, at 80°C, the domains were slightly less spherical.

As a summary, in Figure 11(a), a scheme showing the evolution of morphology in the PMMA-modified epoxy system with precuring temperature is presented. It was evident, therefore, that the next part of the study needed to be to find any kind of relation between the curing conditions (particularly, the temperature), morphology, and properties (particularly, the mechanical properties).

At this point, a theoretical or at least a semiempirical interpretation of the results should be presented. When we took into account the aforementioned, a

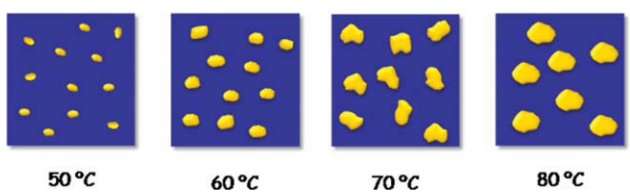

Figure 11 Schematic representation of the morphology dependence with the precuring temperature. [Color figure can be viewed in the online issue, which is available at www.interscience.wiley.com.]

bimodal demixing was expected. However, the results obtained suggest that the domain size was a function of the thermoplastic macromolecules' diffusion rate and, therefore, of the viscosity of the medium.

Let us consider that the conversion for which the phase separation occurs was reached. Then, just in that moment, it is reasonable to think that the system with less viscosity will be that one offering less impediment for the macromolecules to move and that will, therefore, allow a faster growing of the domains. However, during the phase-separation process, there are two factors influencing the viscosity of the system: on the one hand, the temperature itself and, on the other hand, the conversion of the epoxy–amine reaction. A higher temperature had two effects: (1) a direct one with a decrease in the viscosity and (2) an indirect one, which was an increase in the viscosity. Therefore, the domains size should have been a function of the rate at which the thermoplastic molecules were able to diffuse; this rate was the result of the balance between two opposite contributions when the temperature increased: one favorable, due to a simple thermal activation, and the other unfavorable, due to the viscosity increase because the reaction proceeded faster.

The viscosity in a polymeric system has a multivariable dependence on external factors, such as temperature, pressure, and time, and other internal factors, such as the molecular weight, shape of the molecules, and concentration in the case of polymeric solutions. In the system under study, all of them played an important role because it was a reactive mixture changing with time.

The viscosity dependence with temperature is well known to be exponential, as in the case of low-molecular-weight systems:

$$\eta_T = Ae^{-E/RT} \tag{8}$$

where η_T is the temperature dependence of the viscosity (η), R is the universal constant, T the absolute temperature in Kelvin degrees, E is the activation energy for the viscous flow and A is a constant. Therefore, the viscosity decreased with temperature. On the other hand, the viscosity was proportional to the molecular weight, whereas the molecules were small enough because, when the molecular weight was low, the chains could move independently:

$$\eta_M = \eta_T M^i \text{ if } M < M_c \tag{9}$$

where η_M is the molecular weight dependence of the viscosity (η), M is the molecular weight and i is a constant close to 1 when the molecular weight is lower than a critical value (M_c). However, when M increases, the chains entanglements do not allow an independent flow; this yields tensions between them that lead to a viscosity increase. There is a value of M_c for which there is a change in the value of i that is the same for all polymers (3.4):[59]

$$\eta_{M_c} = C(T)M^{3.4} = \eta = Ae^{-E/RT}M^{3.4} \quad \text{If } M > M_c \tag{10}$$

where η_{M_c} represents the molecular weight dependence of the viscosity (η) when the molecular weight of the polymer is greater than the critical value (M_c), $C(T)$ is a constant at a constant temperature. Finally, the addition of one polymer to other should change the viscosity as in the system under study. However, in this case, the concentration was maintained constant, whereas phase separation was not occurring. Taking into account that this process was relatively fast and, when it occurred, the higher fraction was given by the epoxy thermoset component (nearly a 0.8 weight fraction), we assumed that the dependence of the viscosity with concentration must have been negligible.

Considering that M depended on conversion and was the same when phase separation takes place regardless of the precuring temperature (Table I), we concluded that the viscosity of the system, just in the moment of phase separation, was given by eq. (11):

$$\eta_{ps} = Be^{-E/RT} \tag{11}$$

where η_{ps} is the viscosity of the system when phase separation takes place and B is a constant ($B = AM_{ps}^{3.4}$) because the molecular weight just in the moment of phase separation (M_{ps}) is constant.

In Figure 12 (top), the domain size in terms of the domain's $\langle D \rangle$ [$\langle D \rangle$ was calculated with circular domains considered and, therefore, from the values of the average areas ($\langle \text{Area} \rangle$'s) estimated from Fig. 9: $\langle \text{Area} \rangle = \pi(2\langle D \rangle)^2$] as a function of inversed temperature ($1/T$) is presented.

As shown in Figure 12, there was not a linear dependence, which was what was expected if there were a linear relation between $\langle D \rangle$ and Ln η_{ps} as proposed Montarnal et al.[19] in a system based on a DGEBA-type epoxy cured with 1,8-*p*-menthane diamine in the presence of an epoxy-terminated butadiene–acrylonitrile random copolymer. In that study, the average particle size of dispersed domains could be correlated with the viscosity of the system at the cloud point. A straight line with a negative slope was obtained when the natural logarithm of the viscosity at the cloud point versus the $\langle D \rangle$ value of the rubber domains was represented.

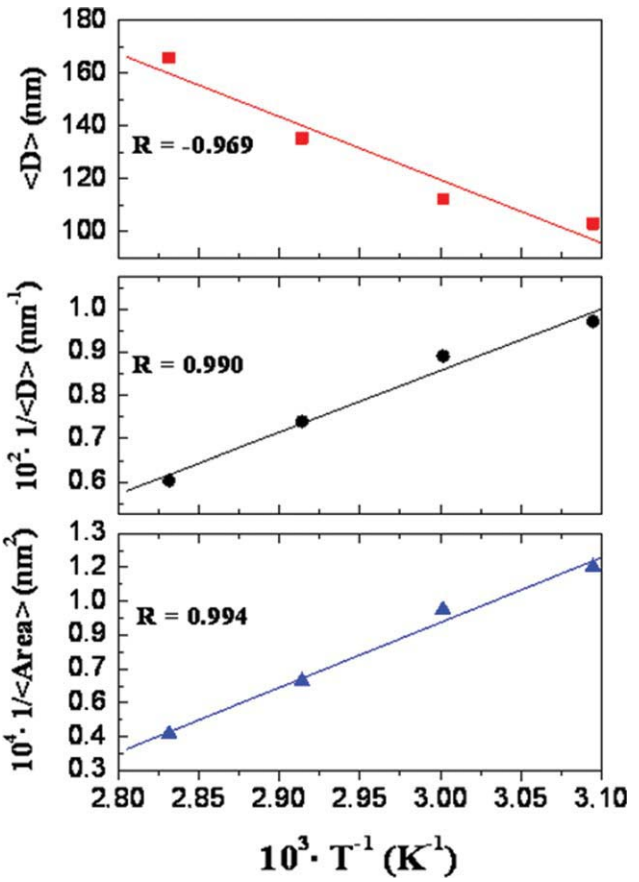

Figure 12 PMMA domain size as a function of the inverse of temperature (see text). [Color figure can be viewed in the online issue, which is available at www.interscience.wiley.com.]

Therefore, another correlation could found that was able to fit better the experimental results. Considering two other possible correlations, $1/\langle D\rangle$ and $1/\langle \text{Area}\rangle$ versus $1/T$ (Fig. 12), we observed better linear fits with correlation coefficients of 0.990 and 0.994, respectively. With eq. (11) taken into account, these results suggest that the area of the domains more than the diameter itself was what showed a correlation with η_{ps} and, particularly, the inverse of the area with the natural logarithm of the inverse of temperature.

With a linear dependence between the inverse of $\langle \text{Area}\rangle$ of the PMMA domains with the inverse of temperature therefore assumed and with consideration of eq. (11), the following expression can be written:

$$\frac{1}{\langle \text{Area}\rangle} = \text{Ln } B + \frac{E}{RT} = \text{Ln}\frac{1}{\eta_{sp}} \tag{12}$$

However, it is necessary to be careful when this expression is used to estimate the morphology because it has at least two limits of applicability: (1) the lower limit, which corresponded in the system under study with the precuring temperature equal to the T_g of the system with 60% epoxy groups conversion (the conversion at which phase separation took place), and (2) the upper limit, which corresponded to that temperature for which the reaction rate was fast enough to entrap the thermoplastic macromolecules before they could segregate into a thermoplastic-rich domain.

Finally, it should be highlighted that only empirical expressions have been tried to predict, within certain limits, the morphology of a thermoplastic-modified epoxy system when the composition was lower than the critical composition, $\Phi_{TP,crit}$. Because of this, greater efforts should be made to determine a theoretical model that could explain or even predict the final morphology in this kind of system.

CONCLUSIONS

In this study, the curing and phase-separation processes of a PMMA-modified epoxy model system were studied. The kinetic analysis of the data obtained by FTIR did not reveal any significant change when 2 wt % PMMA was added to the neat epoxy system. However, the use of fluorescence to monitor the curing process demonstrated that the addition of such a small amount of thermoplastic clearly modified the epoxy–amine reaction. $\langle \nu \rangle$ was very sensitive to physicochemical changes in the system and was clearly more sensitive than FTIR at long curing times. A first attempt to explain the relation between $\langle \nu \rangle$ and the chemical conversion was done. On the basis of the DiBenedetto equation, a semiempirical equation that correlated $\langle \nu \rangle$ with chemical conversion in terms of α was proposed. The model adequately fit both systems (neat and PMMA-modified), which makes it useful for predicting the chemical conversion and the dynamics associated with the system.

On the other hand, this study also presented a deep analysis of the morphologies generated after phase separation. The morphological changes in the PMMA were analyzed in terms of $\langle \text{Area}\rangle$ and the aspect ratio. The curing temperature affected the morphology of the phase-separated system. In particular, the area of the domains of the thermoplastic polymer increased with curing temperature, whereas the SF analysis indicated an increase in the spherical shape of the domains with temperature. These results were interpreted in terms of the viscosity of the reactive mixture. A semiempirical model was proposed, which showed a linear correlation between the inverse of the area of the thermoplastic domains and the inverse of the curing temperature.

References

1. Pascault, J. P.; Verdu, J.; Williams, R. J. J. Thermosetting Polymers; Marcel Dekker: New York,2002.
2. Hedrick, J. L.; Yilgör, I.; Wilkes, G. L.; McGrath, J. E. Polym Bull 1985, 13, 201.
3. Pearson, R. A. In Toughened Plastics. I: Science and Engineering; Riew, C. K.; Kinloch, A. J., Eds.; Advances in Chemistry Series 233; American Chemical Society: Washington, DC, 1993; p 405.
4. Hodgkin, J. H.; Simon, G. P.; Varley, R. J. Polym Adv Technol 1998, 9, 3.
5. Williams, R. J. J.; Rozenberg, R. A.; Pascault, J. P. Adv Polym Sci 1997, 128, 95.
6. Girard-Reydet, E.; Vicard, V.; Pascault, J. P.; Sautereau, H. J Appl Polym Sci 1997, 65, 2433.
7. Ravikumar, H. B.; Ranganathaiah, C.; Kumaraswamy, G. N.; Siddaramaiah, J. J Mater Sci 2005, 40, 6523.
8. Marieta, C.; Remiro, P. M.; Garmendia, G.; Harismendy, I.; Mondragon, I. Eur Polym J 2003, 39, 1965.
9. Schauer, E.; Berglund, L.; Pena, G.; Marieta, C.; Mondragon, I. Polymer 2002, 43, 1241.
10. Soulé, E.; de la Mata, M. G.; Borrajo, J.; Oyanguren, P. A.; Galante, M. J. J Mater Sci 2003, 38, 2809.
11. Riccardi, C. C.; Borrajo, J.; Williams, R. J. J.; Girard-Reydet, E.; Sautereau, H.; Pascault, J. P. J Polym Sci Part B: Polym Phys 1996, 34, 349.
12. Borrajo, J.; Riccardi, C. C.; Williams, R. J. J.; Cao, Z. Q.; Pascault, J. P. Polymer 1995, 36, 3541.
13. Clarke, N.; McLeish, T. C. B.; Jenkins, S. D. Macromolecules 1995, 28, 4650.
14. Gomez, C. M.; Bucknall, C. B. Polymer 1993, 34, 2110.
15. Woo, E. M.; Wu, M. N. Polymer 1996, 37, 2485.
16. Hseih, H. K.; Woo, E. M. J Polym Sci Part B: Polym Phys 1996, 34, 2591.
17. Remiro, P. M.; Riccardi, C. C.; Corcuera, M. A.; Mondragón, I. J Appl Polym Sci 1999, 74, 772.
18. Verchére, D.; Pascault, J. P.; Sautereau, H.; Moschiar, S. M.; Riccardi, C. C.; Williams, R. J. J. J Appl Polym Sci 1991, 42, 701.
19. Montarnal, S.; Pascault, J. P.; Sautereau, H. Rubber-Toughened Plastics; Riew, C. K., Ed.; Advances in Chemistry Series 222; American Chemical Society: Washington, DC, 1989; p 193.
20. López-Quintela, A.; Prendes, P.; Pazos-Pellín, M.; Paz, M.; Paz-Abuín, S. Macromolecules 1998, 31, 4770.
21. Mijović, J.; Andjelić, S. Macromolecules 1995, 28, 2787.
22. Raman, V. I.; Palmese, G. R. Macromolecules 2005, 38, 6923.
23. Mijović, J.; Andjelić, S.; Yee, C. F. W.; Bellucci, F.; Nicolais, L. Macromolecules 1995, 28, 2797.
24. Mikes, F. E.; González-Benito, J.; Llidó, J. B. J Polym Sci Part B: Polym Phys 2004, 42, 64.
25. Olmos, D.; Aznar, A. J.; Baselga, J.; González-Benito, J. J Colloid Interface Sci 2003, 267, 117.
26. Riccardi, C. C.; Fraga, F.; Dupuy, J.; Williams, R. J. J. J Appl Polym Sci 2001, 82, 2319.
27. Roşu, D.; Caşcaval, C. N.; Mustaţà, F.; Ciobanu, C. Thermo Acta 2002, 383, 119.
28. Blanco, M.; Corcuera, M. A.; Riccardi, C. C.; Mondragón, I. Polymer 2005, 46, 7989.
29. Gonzalez-Benito, J.; Esteban, I. Colloid Polym Sci 2005, 283, 559.
30. Francis, B.; Rao, V. L.; vanden Piel, G.; Posada, F.; Groeninckx, G.; Ramaswamy, R.; Thomas, S. Polymer 2006, 47, 5411.
31. González-Benito, J.; Cabanelas, J. C.; Aznar, A. J.; Vigil, M. R.; Bravo, J.; Baselga, J. J Appl Polym Sci 1996, 62, 375.
32. González-Benito, J.; Cabanelas, J. C.; Aznar, A. J.; Vigil, M. R.; Bravo, J.; Baselga, J. J Luminescence 1997, 72–74, 451.
33. González-Benito, J.; Cabanelas, J. C.; Vigil, M. R.; Aznar, A. J.; Bravo, J.; Baselga, J. J Fluoresc 1999, 9, 51.
34. González-Benito, J.; Aznar, A. J.; Lima, J.; Bahía, F.; Maçanita, A. L.; Baselga, J. J Fluorescence 2000, 10, 141.
35. González-Benito, J.; Aznar, A. J.; Baselga, J. J Fluoresc 2001, 11, 307.
36. Loutfy, R. O. Macromolecules 1981, 14, 270.
37. Turrión, S. G.; Olmos, D.; Ekizoglou, N.; González-Benito, J. Polymer 2005, 46, 4023.
38. Leezenberg, P. B.; Frank, C. W. Macromolecules 1995, 28, 7407.
39. Roth, C. B.; McNerny, K. L.; Pager, W. F.; Torkelson, J. M. Macromolecules 2007, 40, 2568.
40. Priestley, R. D.; Ellison, C. J.; Broadbelt, L. J.; Torkelson, J. M. Science 2005, 309, 456.
41. Song, J. C.; Sung, C. S. P. Macromolecules 1993, 26, 4818.
42. Sun, X. D.; Sung, C. P. S. Macromolecules 1996, 29, 3198.
43. Song, J. C.; Neckers, D. C. J Polym Eng Sci 1996, 36, 394.
44. Paczkowski, J.; Neckers, D. C. Macromolecules 1992, 25, 548.
45. Vatanparast, R.; Li, S.; Hakala, K.; Lemmetyinen, H. Macromolecules 2000, 33, 438.
46. Hakala, K.; Vatanparast, R.; Li, S.; Peinado, C.; Bosch, P.; Catalina, F.; Lemmetyinen, H. Macromolecules 2000, 33, 5954.
47. Mikes, F.; González-Benito, J.; Serrano, B.; Bravo, J.; Baselga, J. Polymer 2002, 43, 4331.
48. Strehmel, B.; Strehmel, V.; Younes, M. J Polym Sci Part B: Polym Phys 1999, 37, 1367.
49. Lenhart, J. L.; van Zanten, J. H.; Dunkers, J. P.; Parnas, R. S. Langmuir 2000, 16, 8145.
50. Quirin, J. C.; Torkelson, J. M. Polymer 2003, 44, 423.
51. Olmos, D.; Aznar, A. J.; González-Benito, J. Polym Test 2005, 24, 275.
52. Gonzalez-Benito, J.; Mikes, F.; Bravo, J.; Aznar, A. J.; Baselga, J. J Macromol Sci Phys 2001, 40, 429.
53. Gonzalez-Benito, J.; Mikes, F.; Baselga, J.; Lemmetyinen, H. J Appl Polym Sci 2002, 86, 2992.
54. Rigail-Cedeño, A.; Sung, C. S. P. Polymer 2005, 46, 9378.
55. Olmos, D.; González-Benito, J. Colloid Polym Sci 2006, 284, 654.
56. Pascault, J. P.; Williams, R. J. J. J Polym Sci Part B: Polym Phys 1990, 28, 85.
57. Lakowicz, J. R. Principles of Fluorescence Spectroscopy; Plenum: New York, 1999.
58. Galante, M. J.; Oyanguren, P. A.; Andromaque, K.; Frontini, P. M.; Williams, R. J. J. Polym Int 1999, 48, 642.
59. Cowie, J. M. G. Polymers: Chemistry and Physics of Modern Materials, 3rd ed.; CRC: Boca Raton, FL, 2008.